*Journal of Experimental Botany*, Vol. 68, No. 14 pp. 3829–3839, 2017
doi:10.1093/jxb/erx074 Advance Access publication 28 March 2017

RESEARCH PAPER

# In *Synechococcus* sp. competition for energy between assimilation and acquisition of C and those of N only occurs when growth is light limited

**Zuoxi Ruan[1,2], John A. Raven[3,4] and Mario Giordano[2,5,6,*]**

[1] Marine Biology Institute, Science Center, Shantou University, Shantou, Guangdong 515063, China
[2] Dipartimento di Scienze della Vita e dell'Ambiente, Università Politecnica delle Marche, Ancona 60131, Italy
[3] Division of Plant Sciences, University of Dundee at the James Hutton Institute, Invergowrie, Dundee DD2 5DA, UK
[4] Plant Functional Biology and Climate Change Cluster, University of Technology Sydney, Ultimo NSW 2007, Australia
[5] Institute of Microbiology ASCR, Algatech, Trebon, Czech Republic
[6] National Research Council, Institute of Marine Science, Venezia, Italy

* Correspondence: m.giordano@univpm.it

Received 30 November 2016; Editorial decision 15 February 2017; Accepted 15 February 2017

Editor: Howard Griffiths, University of Cambridge

## Abstract

**The carbon-concentrating mechanisms (CCMs) of cyanobacteria counteract the low $CO_2$ affinity and $CO_2$:$O_2$ selectivities of the Rubisco of these photolithotrophs and the relatively low oceanic $CO_2$ availability. CCMs have a significant energy cost; if light is limiting, the use of N sources whose assimilation demands less energy could permit a greater investment of energy into CCMs and inorganic C (Ci) assimilation. To test this, we cultured *Synechococcus* sp. UTEX LB 2380 under either N or energy limitation, in the presence of $NO_3^-$ or $NH_4^+$. When growth was energy-limited, $NH_4^+$-grown cells had a 1.2-fold higher growth rate, 1.3-fold higher dissolved inorganic carbon (DIC)-saturated photosynthetic rate, 19% higher linear electron transfer, 80% higher photosynthetic 1/$K_{1/2}$(DIC), 2.0-fold greater *slope* of the linear part of the photosynthesis versus DIC curve, 3.5-fold larger intracellular Ci pool, and 2.3-fold higher Zn quota than $NO_3^-$-grown cells. When energy was not limiting growth, there were not differences between $NH_4^+$- and $NO_3^-$-grown cells, except for higher linear electron transfer and larger intracellular Ci pool.**
**We conclude that, when energy limits growth, cells that use the cheaper N source divert energy from N assimilation to C acquisition and assimilation; this does not happen when energy is not limiting.**

**Key words:** Ammonium, $CO_2$ concentrating mechanisms (CCMs), cyanobacteria, internal carbon pool, nitrate.

## Introduction

Algae have developed mechanisms that increase the concentration of $CO_2$ in the proximity of Rubisco, the so-called $CO_2$ concentrating mechanisms (CCMs), in response to a general downward trend over the last 2 billion years in the environmental $CO_2$ concentration and $CO_2$ to $O_2$ ratio (Giordano *et al.*, 2005). The Rubisco of cyanobacteria (Form 1A in α-cyanobacteria; Form 1B in β-cyanobacteria) is characterized by an especially low ability to discriminate in favour of $CO_2$ over $O_2$ and by a rather high $K_{1/2}(CO_2)$ (105–750 μM) (Badger *et al.*, 1998; Scott *et al.*, 2007; Price *et al.*, 2008), only paralleled by the

Form II Rubisco of peridinin-containing core dinoflagellates. Diffusive $CO_2$ entry, at the present atmosphere-equilibrium $CO_2$, could not support photosynthesis with the observed Rubisco kinetics in cyanobacteria; to cope with these difficulties, all photosynthetically competent cyanobacteria have CCMs that can accumulate $CO_2$ in intracellular carboxysomes up to one thousand times the concentration in the environment (Badger and Andrews, 1982; Miller *et al.,* 1988; Tortell, 2000 and references therein; Raven *et al.,* 2012).

Cyanobacterial CCMs are energized by linear and cyclic electron transport (Mi *et al.,* 1992; Mi *et al.,* 1995; Li and Canvin, 1998; Zhang *et al.,* 2004; Fukuzawa *et al.,* 2012). Both linear and cyclic electron transport produce an $H^+$ gradient across the thylakoid membrane that is essential for the formation of ATP, which fuels the BCT1 bicarbonate transporter (an ATP-binding cassette type of transporter) directly (Omata *et al.,* 1999). This ATP may also indirectly provide the energy required by the $Na^+$-dependent SbtA and BicA $HCO_3^-$ transporters (Shibata *et al.,* 2002; Price *et al.,* 2004; Fukuzawa *et al.,* 2012). The $CO_2$ that enters the cytosol can be unidirectionally converted to $HCO_3^-$ by the NDH-$1_3$ (on the thylakoids) and NDH-$1_4$ (on the plasmalemma) complexes, using energy derived from electron transport through the NDH-1 complexes (NADPH-plastoquinone oxidoreductase) (Price, 2011). The cytosolic $HCO_3^-$ moves through anion-selective pores in the proteinaceous coat of the carboxysomes (Kerfeld *et al.,* 2005) to the carboxysome lumen that contains most of the carbonic anhydrase (CA) and Rubisco activities in the cell and that, thanks to the balance between these two enzymatic activities, is characterized by a high steady-state $CO_2$ concentration. The ensemble of $HCO_3^-$ transporters (BCT1, SbtA, BicA; not all necessarily present in all cyanobacteria), facilitators of $CO_2$ diffusion, and the energized converters of $CO_2$ to $HCO_3^-$ (NDH-$1_{3/4}$) and carboxysomes with their enzymatic complement constitute the CCMs of cyanobacteria and are necessary for the fixation of $CO_2$ by Rubisco at present day $CO_2$ concentrations. Energy is required to maintain the high steady-state cytosolic and intracarboxysomal inorganic carbon (Ci) concentration against the cytosol/extracellular $HCO_3^-$ electrochemical potential difference. The gradient driving diffusive $CO_2$ entry is provided by $CO_2$ consumption by NDH-$1_3$ and NDH-$1_4$. Energy is also needed for the very small Rubisco oxygenase activity and consequent photorespiratory pathway that occurs in cyanobacteria despite the occurrence of the CCM (Raven and Lucas, 1985; Raven *et al.,* 2012).

It has been estimated that, at steady state, the costs of Ci transport could be as high as 18–40% of the total energy needed to fix one carbon atom (Fu and Han, 2010). Using a different approach, Raven *et al.,* (2014) showed that the minimum cost of $CO_2$ fixation, when $CO_2$ saturates Rubisco, is 9 absorbed photosynthetically active radiation (PAR) photons per $CO_2$ converted to triose phosphate. Raven *et al.,* (2014) also estimated that the minimum energy cost of $HCO_3^-$ accumulation is 0.5 absorbed PAR photons per $HCO_3^-$ accumulated, assuming no leakage; that is, an extra 5.5% must be added to the cost of $CO_2$ assimilation by Rubisco. This applies to both the active transport of $HCO_3^-$ and the passive entry of $CO_2$ followed by the energized conversion of $CO_2$ to $HCO_3^-$. Table 1 in the supplementary information of Raven and Beardall (2016) summarizes the literature information on Ci leakage in cyanobacteria and shows that such leakage can vary from 9 to 92% of the total $HCO_3^-$ accumulated in the cell. The cost of $HCO_3^-$ pumping is thus 5.3–58% of the total cost of $CO_2$ assimilation plus $HCO_3^-$ pumping.

The energy needed for CCM maintenance derives, directly or indirectly, from photosynthesis (Kaplan *et al.,* 1987; Spiller *et al.,* 1988), which in turn depends on the photon flux density (Kaplan *et al.,* 1987; Kübler and Raven, 1994, 1995; Bartual and Gálvez, 2002). CCM activity is controlled by light, and sub-saturating irradiances result in a lower affinity of cells for Ci (Beardall, 1991; Poza-Carrión *et al.,* 2001; de Araujo *et al.,* 2011) and a decreased ratio of internal to external Ci concentrations in *Anabaena* (Beardall, 1991) and *Leptolyngbya* (de Araujo *et al.,* 2011). In *Anabaena* (Beardall, 1991) and *Leptolyngbya* (de Araujo *et al.,* 2011), the intracellular accumulation of Ci increased with irradiance up to a certain photon flux; at higher irradiances, the CCM functions as a energy dissipater, with a larger fraction of the Ci pumped by the CCM lost as $CO_2$ efflux from the cell (Salon *et al.,* 1996; Tchernov *et al.,* 1997, 2003; Qiu and Liu, 2004; de Araujo *et al.,* 2011).

The nitrogen source may affect Ci uptake (Giordano and Bowes, 1997; Beardall and Giordano, 2002; Raven *et al.,* 2011; Raven and Beardall, 2014) and assimilation (Lawrie *et al.,* 1976; Coronil *et al.,* 1993; Huppe and Turpin, 1994; Kaplan *et al.,* 1998). The cost of the assimilation of one mole of $NO_3^-$, a major source of N in oceanic waters, into glutamate, with 2-oxoglurarate as the C skeleton, is 5 moles of NADPH and 1 mole of ATP (Noctor and Foyer, 1998; Ruan and Giordano, 2017). If N is available as $NH_4^+$, its assimilation costs 1 mole of NADPH and 1 mole of ATP per glutamate produced, although additional costs are needed to minimize the potential toxicity of this N form at high concentration (Huppe and Turpin, 1994; Noctor and Foyer, 1998; Stitt and Krapp, 2002). This difference in assimilation cost can affect photosynthetic performance. Photosynthesis is typically saturated by a lower irradiance in the presence of $NH_4^+$ than in the presence of $NO_3^-$ (Lara and Romero, 1986). Under low light, $CO_2$ fixation by the cyanobacterium *Anacystis nidulans* was depressed if $NO_3^-$ was added to N-starved cultures, whereas the opposite was true if $NH_4^+$ was added. In *Synechococcus* UTEX LB 2380, using the rather indirect $^{18}O$ and $^{13}C$ dissolved inorganic carbon (DIC) light/dark method, a greater accumulation of $CO_2$ was observed in the absence of N than in the presence of complex N (Spiller *et al.,* 1988), suggesting that the energy saved from N assimilation can indeed be used for Ci assimilation. The N source also appears to affect CCM activity in eukaryotic green algae: *Dunaliella salina* cells cultured in the presence of $NH_4^+$ had a higher photosynthetic affinity for $CO_2$ than cells grown on $NO_3^-$ (Giordano and Bowes, 1997; Giordano, 2001; Beardall and Giordano, 2002). Recent research showed a cooperative regulation of bicarbonate transport by C and N in the diazotrophic cyanobacterium *Anabaena* strain (López-Igual *et al.,* 2012). Concerted changes in transcripts related to

C assimilation were observed in *Synechococcus* sp. PCC 7002 when different N sources were supplied: the expression of the SbtA $Na^+$-dependent $HCO_3^-$ transporter was about three times higher in $NH_4^+$-grown cells than in $NO_3^-$-grown cells; a similar effect was observed for the transcript of $CO_2$ diffusion facilitator NDH-$1_3$ (Ludwig and Bryant, 2012).

CAs are Zn (mostly) enzymes often involved in biophysical CCMs (Giordano *et al.,* 2005). In cyanobacterial cells, they are among the most abundant Zn enzymes (Cavet *et al.,* 2003). Cyanobacterial CAs are mostly associated with carboxysomes: a β-carbonic anhydrase (CsoSCA) is present in α-carboxysome and a γ-carbonic anhydrase (CCmM) is a component of β-carboxysomes (Kerfeld and Melnicki, 2016; McGurn *et al.,* 2016; DiMario *et al.,* 2017). Extracellular CAs have also been found in *Microcoleus* from stromatolites (Kupriyanova *et al.,* 2007) and extracellular CA activity has been detected in the desert species *Nostoc flagelliforme* (Ye *et al.,* 2008). If a conspicuous up-regulation of CCM occurs in the presence of $NH_4^+$ rather than $NO_3^-$, we would expect the abundance of CA to increase and, consequently, that of its metal cofactor, Zn. The Zn cell quota may thus constitute a relatively easy-to-measure, although approximate, proxy for CCM activity. Similarly, Fe, which is abundant in the electron transport chain (especially in the cytochrome b6/f and PSI complexes) can be used as a proxy for the abundance of proteins involved in this part of the photosynthetic apparatus (although Fe is much more spread across cell metal-proteins). The cell quotas of Zn and Fe may therefore contribute to (crudely) determining the relative changes in the portion of the proteome associated with the CCM and photosynthetic machinery.

Based on the above, we hypothesized that when energy is limiting and N is sufficient, the use of $NH_4^+$ rather than $NO_3^-$ makes more energy available for C acquisition (and assimilation) and a higher CCM activity and intracellular DIC concentration can be sustained. Higher CCM activity could support a higher photosynthetic rate.

The experiments involved *Synechococcus* UTEX LB 2380 that was isolated at an unknown date from the coastal ocean of Palau, 3–9° N, 131–135° E, which has a mean annual temperature of 27°C (Watanabe *et al.,* 2006; Neall and Trewick, 2008). The concentrations of inorganic combined N at the site of isolation are 0.04–0.13, 0.01–0.05, and 0.33–0.38 μmol $kg^{-1}$ of water for $NO_3^-$, $NO_2^-$ and $NH_4^+$, respectively (Watanabe *et al.,* 2006). Waters of the coastal reef have almost 0.2 units lower pH than open ocean seawater, with a corresponding 9–14% higher dissolved $CO_2$ concentration (Watanabe *et al.,* 2006; Shamberger *et al.,* 2014). We could not find data on vertical mixing or turbidity in the coastal waters of Palau, so could not determine mean photon flux density; hence, it is not certain whether light or nutrients limit the growth of *Synechococcus* UTEX LB 2380 at its isolation site.

## Materials and methods

### *Culture conditions*

The non-diazotrophic coastal cyanobacterium *Synechococcus* UTEX LB 2380 was cultured in the artificial seawater medium AMCONA (Artificial Multipurpose Complement for the Nutrition of Algae; buffered at a final pH of 8.25 with 10 mM Tris), at 25°C. The AMCONA medium contains 550 μM $NO_3^-$; for our experiments we also modified AMCONA by using $NH_4^+$ in the place of $NO_3^-$ at the same N concentration of the original recipe or by using either $NH_4^+$ or $NO_3^-$ at a lower concentration (22 μM). The growth irradiance was 100 μmol photons·$m^{-2}$·$s^{-1}$ (12 h light:12 h dark), which limits growth at 550 μM N and saturates growth at 22 μM, regardless of the N form (Ruan and Giordano, 2017). Cultures were maintained in 250 mL Erlenmeyer flasks containing 200 mL of alga suspension.

The identification of the energy- and N-limited conditions was performed in batch cultures, after an acclimation period of at least eight generations in each growth regime. The carbonate system of the growth media is shown in Supplementary Table S1 (available at *JXB* online). For all other experiments, cells were grown semi-continuously at dilution rates corresponding to the maximum growth rate of batch cultures in each experimental condition. The semi-continuous cultures were maintained in each growth regime for at least 10 generations prior to any measurement.

### *Carbonate system of the growth media*

DIC concentration was measured with an infrared gas analyser (IRGA; LI-COR LI840A, LI-COR Biosciences, Lincoln, NE, USA). A 20 mL aliquot of culture media was put into a gas-tight glass chamber (mixing chamber) and gassed with a carrier gas (pure $N_2$), which was treated with soda lime before entering the chamber to trap any residual $CO_2$. A predetermined small volume of 4 M HCl was added to the mixing chamber to bring the medium pH to about 1.0 and convert all DIC to $CO_2$. The gas exiting the mixing chamber, constituting the sole carrier gas for the blank measurements or the carrier gas enriched with the $CO_2$ produced by medium acidification for the sample measurements, reached the IRGA after dehydration through silica gel and its $CO_2$ content was determined.

The total DIC concentration determined with the IRGA and the pH of the medium were entered into the CO2SYS software (Lewis *et al.,* 1998) to estimate the DIC speciation. For the calculations, the following constants were chosen: $K_1$ and $K_2$ carbonate dissociation constants from Roy *et al.,* (1993); standard acidity constant of $HSO_4^-$ from Dickson (1990); and the $K_{p1}$, $K_{p2}$, and $K_{p3}$ dissociation constant of phosphoric acid and $K_{Si}$ dissociation constant of silicic acid from Millero (1995).

### *Electron transfer*

Electron transfer was studied with a DUAL PAM 100 (Heinz Walz GmbH, Effeltrich, Germany). Cells were harvested by centrifugation (J2-HC centrifuge, Beckman Coulter, Brea, CA, USA) at 9000 *g* for 20 min; 2 mL of cell suspension with ~18 μg Chl *a*·$mL^{-1}$ was obtained and used for the measurements.

The quantum yields of PSI and PSII were assessed as detailed previously (Klughammer and Schreiber, 1994; Pfündel *et al.,* 2008; Schreiber and Klughammer, 2008) after 10 min of dark acclimation, as described by Ratti *et al.,* (2011). The maximum P700 absorbance of the near-infrared, *P*m, occurred after pre-illumination using far-red light and at the onset of a saturated pulse when the electron transfer chain was fully oxidized. *P*o, the minimum P700 signal, was determined after the cessation of the saturated pulse, when the PSI centres were completely reduced. *P*m' was the maximum PSI absorbance produced in the presence of actinic light by a saturation pulse. All other parameters were derived from these three measurements.

The relative electron transfer rate (rETR) versus irradiance curves (rapid light curves) were carried out according to Fanesi *et al.,* (2014) in the irradiance range 0–3500 photons·$m^{-2}$·$s^{-1}$. The curves were fitted with the Origin 7.0 SR0 software (OriginLab Corporation, Northampton, MA, USA) using the following model from Walsby (1997):

$$P = Pm\left(1-\exp\left(\alpha I / Pm\right)\right) + \beta I,$$

where $P$ is the rETR at irradiance $I$; $P$m is the maximum rETR; $\alpha$ is the maximum quantum efficiency of electron transfer; and $\beta$ is the slope of the curve at high irradiances, which is negative if there is photoinhibition.

We are aware of the caveats of ETR measurements, especially in the case of cyanobacteria. Even absolute ETR measurements, allowing for photon absorptance, do not match completely with other methods of determining photosynthesis (Suggett *et al.,* 2003; 2009), and cyanobacteria may pose particular problems (Campbell *et al.,* 1998; Acuña *et al.,* 2016). However, this appeared to be the most direct way to assess energy partitioning within the photosynthetic apparatus. Also, we used these data conservatively and mostly just to confirm the results obtained by other methods.

### *Inhibitor treatment*

Two inhibitors were used to study electron transfer in *Synechococcus* UTEX LB 2380: 3-(3,4-dichlorophenyl)-1,1-dimethylurea (DCMU), which blocks the electron flow between the quinone pockets $Q_A$ and $Q_B$ in PSII, and 2,5-dibromo-6-isopropyl-3-methyl-1,4-benzoquinone (DBMIB), which inhibits the re-oxidation of plastoquinols by the cytochrome $b_6f$ complex and blocks electron transfer to PSI. The inhibitors were used at the minimum effective concentration, which was determined in preliminary tests on $O_2$ evolution. DCMU was used at a final concentration of 5 µM and DBMIB was used at a final concentration of 10 µM.

### *Measurement of $O_2$ evolution rates as a function of dissolved inorganic carbon*

Growth medium deprived of Ci (DIC-free) was freshly prepared before starting the measurements with the following procedure: 10 mL AMCONA medium was acidified to pH 1.6 with 150 µL of 1 M HCl; at this pH, all DIC was converted to $CO_2$. The acidified medium was then bubbled with $N_2$ for ~60 min to purge out gaseous $CO_2$. Pre-weighed NaOH pellets, carefully rinsed with 0.1 M HCl (to eliminate Ci from their surface), were used to bring the pH back to growth pH (8.25). Cells ($3–8 \times 10^7$) were harvested by centrifugation at 4400 *g* for 10 min, washed twice with freshly prepared DIC-free AMCONA medium, and finally resuspended in 2 mL of the same medium. This algal suspension was bubbled with $N_2$ in a Clark type oximeter chamber (Chloroview 2, Hansatech, King's Lynn, UK) to lower the $O_2$ concentration to 0; the chamber was then closed and illuminated at growth (100 µmol photons·m$^{-2}$·s$^{-1}$) or saturating (465 µmol photons·m$^{-2}$·s$^{-1}$) irradiance. Photosynthesis was allowed to take place until the residual carbon was consumed and the $O_2$ evolution compensation point for $CO_2$ was reached. Typically, at this point the $O_2$ concentration would be ~20% of saturation. $O_2$ evolution rates were then measured as a function of DIC by adding incremental $NaHCO_3$ concentrations until saturation was reached; after saturation, at least three more $NaHCO_3$ additions were made to ensure that the saturation phase of the curve could be properly modelled. $NaHCO_3$ solution was added every 60 s within the range 5–25 µM (final $NaHCO_3$ in the $O_2$ electrode chamber), and every 30 s for concentration above 25 µM. The volume increase due to $NaHCO_3$ addition (~1.5%) was considered in the calculation of the concentrations. The buffer in the medium maintained the pH at 8.25 throughout the measurement. Photosynthetic $O_2$ evolution was recorded using LabVIEW 2008 (National Instruments, Milano, Italy). Dark respiration rates were determined following photosynthesis measurements, between 1 and 5 min after the light had been switched off.

The photosynthesis versus DIC curves were modelled to a Michaelis–Menten (1913) kinetics, using the following equation:

$$P = P\mathrm{m}(\mathrm{DIC} / (\mathrm{K}_{1/2}(\mathrm{DIC}) + \mathrm{DIC})),$$

where DIC is the concentration of dissolved inorganic carbon, $P$m is the DIC-saturated photosynthetic rate, and $K_{1/2}$(DIC) is the Michaelis–Menten constant.

### *Internal inorganic carbon pool*

The silicone oil centrifugation technique was used to estimate the Ci accumulation, the internal pH, and the internal cell volume as described by Ratti *et al.,* (2007). The only difference was that the cell suspension used for the silicone oil assay contained $5.7–9.8 \times 10^7$ cells·mL$^{-1}$.

### *Iron and zinc determination*

Iron and zinc cell contents were measured by total reflection X-ray fluorescence spectrometry (picofox S2; Bruker AXS Microanalysis GmbH, Ettlingen, Germany), according to Fanesi *et al.,* (2014)

### *Statistical analysis*

All data are presented as the means and standard deviations of three replicate measurements obtained from three independent cultures. $K_{1/2}$(DIC) and $P$m were derived from a double-reciprocal plot, which was fitted with a linear model; the determination coefficients ($R^2$) of the goodness-of-fit of these models are reported in Supplementary Table S2 (available at *JXB* online). The same statistical treatment was applied to the slopes of the DIC-limited parts of the photosynthesis versus DIC curves (at least six data points); these $R^2$ values are also shown in Supplementary Table S2. For the ratios of the Fe and Zn contents, standard deviations were obtained by error propagation (Taylor, 1997). The significance of variance was assessed by two-tailed *t*-test performed with the Origin 7.0 SR0 software (OriginLab Corporation) or by two-way ANOVA analysis followed by Student–Newman–Keuls multiple comparison test, performed using GMAV 5.0 for Windows XP (by A.J. Underwood and M.G. Chapman, Institute of Marine Ecology, The University of Sydney, Australia). In the two-way ANOVA, the significance of homogeneity of variance was always checked by Cochran's test before analysis; if the results of this test were not satisfactory, data were transformed until the homogeneity of variance was obtained. The level of significance was always set at 5%.

## Results

### *Growth*

The identification of the N-limiting and N-sufficient conditions was performed in batch cultures (Fig. 1). Cells had similar growth rates in $NO_3^-$ and in $NH_4^+$ when the N concentration was <550 µM; above this N concentration, growth

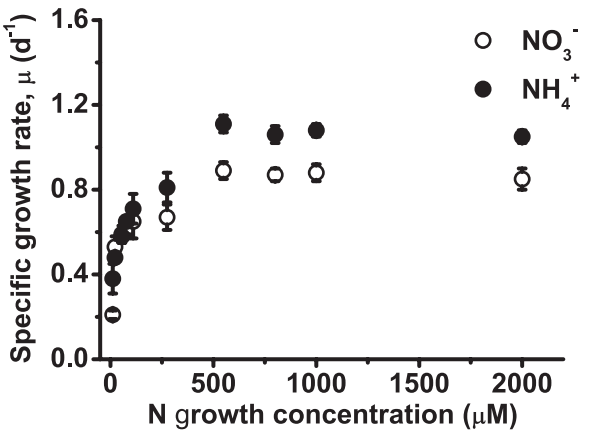


**Fig. 1.** Growth as a function of inorganic N concentration of *Synechococcus* sp. UTEX LB 2380 acclimated to either $NO_3^-$ or $NH_4^+$, at an irradiance of 100 µmol photons·m$^{-2}$·s$^{-1}$. The error bars indicate the standard deviations ($n$ = 3).

was faster when N was supplied as $NH_4^+$ rather than as $NO_3^-$ (Fig. 1; *t*-test, $P < 0.01$).

That high N-grown cells were energy (light)-limited was demonstrated by the fact that increased irradiance elicited a higher growth rate above N saturation (550 µM); the same was not true if N did not saturate growth. These data have been previously published in Ruan and Giordano (2017).

Based on the exponential growth rates in batch cultures, the following dilution rates were chosen for the semi-continuous cultures: 0.40 $day^{-1}$ at 22 µM $NO_3^-$, 0.35 $day^{-1}$ at 22 µM $NH_4^+$, 0.60 $day^{-1}$ at 550 µM $NO_3^-$, and 0.67 $day^{-1}$ at 550 µM $NH_4^+$.

### *Photosynthetic $O_2$ evolution versus dissolved inorganic carbon curves*

Under N-sufficient conditions (limiting energy), the DIC-saturated photosynthetic rates of $NH_4^+$-grown cells were 1.3- and 1.7-fold those of $NO_3^-$-grown cells, respectively, at 100 µmol photons·$m^{-2}$ $s^{-1}$ and 465 µmol photons·$m^{-2}$·$s^{-1}$. The photosynthetic DIC affinity of $NH_4^+$-grown cells measured as $1/K_{1/2}$(DIC) was 1.8-fold (at 100 µmol photons·$m^{-2}$·$s^{-1}$) and 2.3-fold (at 465 µmol photons·$m^{-2}$·$s^{-1}$) higher than those of the $NO_3^-$-grown counterpart. The *slope* of the linear portion of the *P* versus DIC curve was 2.0- and 2.4-fold higher than those of $NO_3^-$-grown cells at 100 and 465 µmol photons·$m^{-2}$·$s^{-1}$, respectively (Fig. 2; Table 1). When N limited growth, there was no significant difference between the photosynthetic affinities for DIC of cells grown on different N sources at growth irradiance (Fig. 2; Table 1). When the irradiance was increased to 465 µmol photons·$m^{-2}$·$s^{-1}$, the DIC-saturated photosynthetic $O_2$ evolution rate and the photosynthetic affinity for DIC of energy-limited cells increased (Fig. 2; Table 1). In N-limited cells, an increase of irradiance increased $1/K_{1/2}$(DIC) but had no effect on the photosynthetic rate at saturating DIC (Table 1).

### *Intracellular inorganic carbon pool*

Compared with $NO_3^-$-grown cells, the pool size of cells grown on $NH_4^+$ was about 3.0-fold higher in N-limited cells and 3.6-fold higher in energy-limited cells (Fig. 3). The DIC concentration factor (DIC inside/DIC outside) was 3.1- and

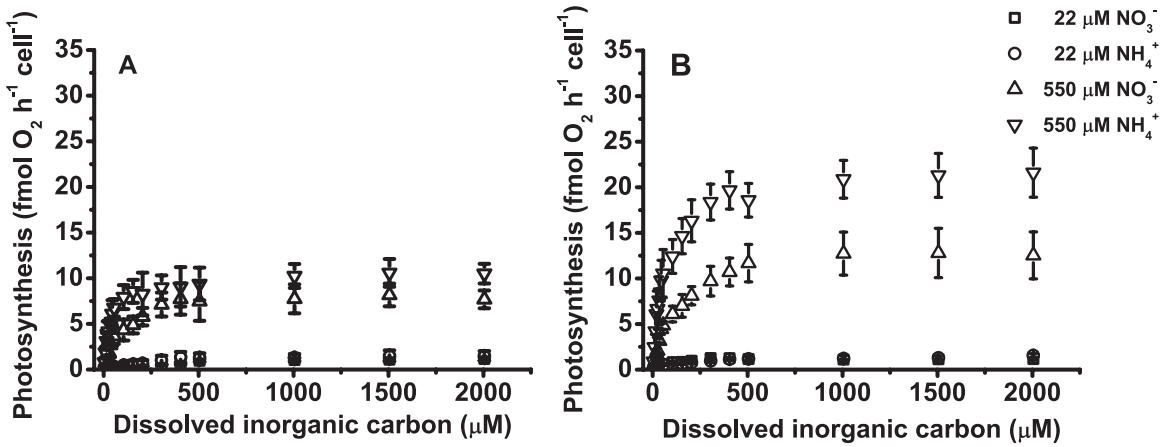


**Fig. 2.** Photosynthetic rates as a function of DIC concentration under (**A**) growth irradiance (100 µmol photons·$m^{-2}$·$s^{-1}$) and (**B**) at growth-saturating irradiance (465 µmol photons·$m^{-2}$·$s^{-1}$) for *Synechococcus* sp. UTEX LB 2380 acclimated to 22 µM (N-limited) or 550 µM (energy-limited) $NO_3^-$ or $NH_4^+$. The error bars indicate the standard deviations ($n = 3$).

**Table 1.** *Parameters obtained from the photosynthesis versus DIC curves at growth irradiance (100 µmol photons·$m^{-2}$·$s^{-1}$) and at growth-saturating irradiance (465 µmol photons·$m^{-2}$·$s^{-1}$) for* Synechococcus *sp. UTEX LB 2380 acclimated to either 22 µM (N-limited) or 550 µM (energy-limited) $NO_3^-$ or $NH_4^+$*

*Pm* is the DIC-saturated photosynthetic rate (fmol $O_2$·$cell^{-1}$·$h^{-1}$); $1/K_{1/2}$(DIC) ($\mu M^{-1}$) is the reverse of the Michaelis–Menten constant and an indication of affinity; *slope* is the slope of the DIC-limited part of the photosynthesis versus DIC curve (fmol $O_2$·$cell^{-1}$·$h^{-1}$/ µM DIC). The values are shown as mean ± standard deviation ($n = 3$). Different letters denote significantly different means ($P < 0.05$)

| Photosynthetic parameters | Irradiance | C affinity and DIC-saturated photosynthesis | | | |
|---|---|---|---|---|---|
| | | N-limited cells | | Energy-limited cells | |
| | | $NO_3^-$ | $NH_4^+$ | $NO_3^-$ | $NH_4^+$ |
| $1/K_{1/2}$(DIC) | 100 | $0.009^a$ ± 0.002 | $0.010^a$ ± 0.001 | $0.010^b$ ± 0.0062 | $0.016^b$ ± 0.003 |
| | 465 | $0.020^a$ ± 0.005 | $0.017^a$ ± 0.003 | $0.011^b$ ± 0.002 | $0.024^a$ ± 0.004 |
| *Slope* | 100 | $0.003^a$ ± 0.002 | $0.006^a$ ± 0.004 | $0.060^b$ ± 0.009 | $0.117^c$ ± 0.021 |
| | 465 | $0.013^a$ ± 0.004 | $0.011^a$ ± 0.003 | $0.094^b$ ± 0.011 | $0.229^c$ ± 0.079 |
| *Pm* | 100 | $1.26^a$ ± 0.31 | $1.50^a$ ± 0.53 | $7.86^b$ ± 0.26 | $10.50^c$ ± 1.08 |
| | 465 | $1.16^a$ ± 0.11 | $1.30^a$ ± 0.21 | $12.5^b$ ± 2.58 | $21.6^c$ ± 2.69 |

3.5-fold higher in $NH_4^+$-grown cells than in $NO_3^-$-grown cells at 22 and 550 µM N, respectively (Table 2). The N chemical form also affected the intracellular pH ($P < 0.01$), which was higher in the presence of $NH_4^+$ than in $NO_3^-$, although the difference was statistically significant only when energy was limiting for growth (Table 2).

### *Iron and zinc cell quotas*

The cell quotas of Fe and Zn were unaffected by the N form used for growth when N was limiting. When growth was limited by energy, both metals were about 2-fold more abundant in $NH_4^+$-grown cells (Fig. 4)

### *Electron transfer*

#### *PSII*

The relative maximum electron transfer rate at PSII, $rETR(II)_{max}$, was somewhat higher with limiting N than with limiting energy, as was the slope of the linear part of the curve ($\alpha$) (Table 3; Supplementary Figs S1 and S2, available at *JXB* online). The irradiance at which the onset of saturation occurred ($E_k$) was similar under both types of limitations and N sources. Photoinhibition was observed only in N-limited cells beyond ~1500 µmol photons·m$^{-2}$·s$^{-1}$. In all cases, the N source had no significant influence on the electron transfer

**Table 2.** *$CO_2$ and DIC concentration factors (relative to the external medium) and intracellular pH of* Synechococcus *sp. UTEX LB 2380 acclimated to N- or energy-limited conditions, in the presence of either $NO_3^-$ or $NH_4^+$, at an irradiance of 100 µmol photons·m$^{-2}$·s$^{-1}$*

The measurements were conducted in the presence of 0.11 mM DIC (0.56 µM $CO_2$), at the external pH of 8.30. The values are shown as mean ± standard deviation ($n$ = 3–4). Different letters denote significantly different means ($P < 0.05$).

| | N-limited cells | | Energy-limited cells | |
|---|---|---|---|---|
| | $NO_3^-$ | $NH_4^+$ | $NO_3^-$ | $NH_4^+$ |
| Intracellular pH | $7.68^{ab}$ ± 0.21 | $7.88^{b}$ ± 0.17 | $7.57^{a}$ ± 0.05 | $7.93^{b}$ ± 0.06 |
| DIC concentration factor | $11.4^{a}$ ± 4.30 | $34.9^{b}$ ± 6.10 | $8.80^{a}$ ± 1.50 | $31.0^{b}$ ± 5.20 |
| $CO_2$ concentration factor | $53.0^{ab}$ ± 19.6 | $99.8^{c}$ ± 17.3 | $52.8^{a}$ ± 9.00 | $78.4^{bc}$ ± 13.0 |

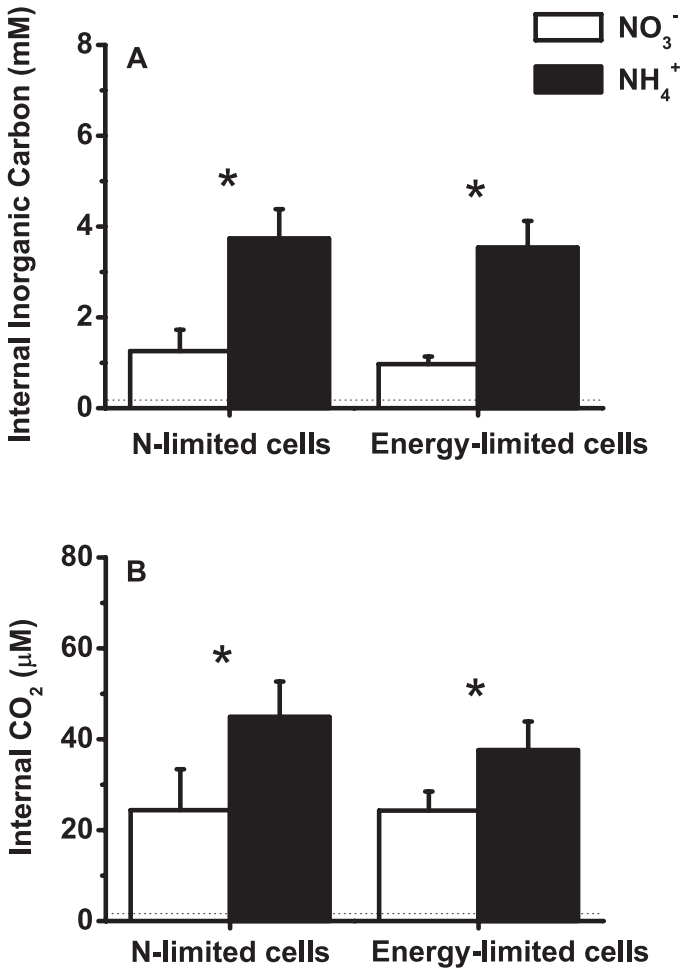


**Fig. 3.** (**A**) Internal total DIC and (**B**) internal $CO_2$ concentrations of *Synechococcus* sp. UTEX LB 2380 acclimated to either N- or energy-limited conditions, in the presence of either $NO_3^-$ or $NH_4^+$ as the sole N source. The dotted lines represent the external concentration of 0.11 mM DIC (A) and 0.56 µM $CO_2$ (B). The asterisks represent significant difference between treatments ($P < 0.05$). The error bars indicate the standard deviations ($n$ = 3–4).

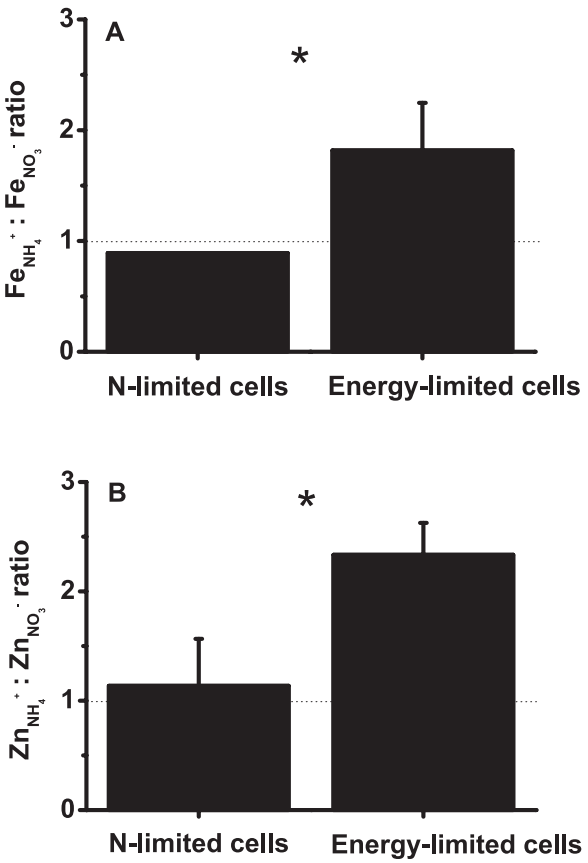


**Fig. 4.** Content of (**A**) Fe and (**B**) Zn in $NH_4^+$-grown cells relative to those in $NO_3^-$-grown cells of *Synechococcus* sp. UTEX LB 2380 acclimated to either N- or energy-limited conditions. The asterisks represent a significant difference between treatments ($P < 0.05$). The error bars indicate the standard deviations ($n$ = 3).

through PSII. As expected, the application of DCMU prevented electron transfer at PSII (Supplementary Figs S1 and S2).

*PSI*

The relative maximum electron transfer rate at PSI, rETR(I)$_{max}$ was unaffected by the N source in N-limited cells, which had an appreciably lower transfer rate than energy-limited cells (Table 4; Supplementary Figs S1 and S2). Furthermore, energy-limited cells showed a stimulation of rETR(I)$_{max}$ when $NH_4^+$ was the N source. The value of $\alpha$ was also unaffected by the N source in N-limited cells, which had a higher affinity for photons than their energy-limited counterparts. The energy-limited cells also showed a differential response to the N sources for $\alpha$, which in $NO_3^-$ was ~80% that in $NH_4^+$. $E_k$ was ≥2-fold higher in energy-limited than in N-limited cells, but did not show any obvious trend with respect to the N form.

When DCMU was applied to the cells, all PSI parameters decreased substantially (Table 4). The electron transfer through PSI of N-limited cells did not show any appreciable difference between $NO_3^-$- and $NH_4^+$-grown cells for all parameters. In the case of energy-limited cells, interestingly, DCMU treatment elicited an effect by the N source on the rETR(I): in this treatment, both energy- and N-limited cells had a lower ETR(I) if N was supplied as $NH_4^+$ (Table 4). DCMU also exacerbated the difference between energy-limited $NO_3^-$- and $NH_4^+$-grown cells in the affinity for photons (Table 4). The use of DBMIB, after DCMU, eliminated electron transfer through PSI (Supplementary Figs S1, S2, and S3, available at *JXB* online).

**Table 3.** *Kinetic parameters of the rETR(II) versus irradiance curves of* Synechococcus *sp. UTEX LB 2380 acclimated to growth in N- or energy-limited conditions, in the presence of either $NO_3^-$ or $NH_4^+$, at an irradiance of 100 µmol photons·m$^{-2}$·s$^{-1}$*

rETRmax, maximum relative electron transport; $\alpha$, slope of the light-limited portion of the rETR versus irradiance curve; $E_k$ (µmol photons·m$^{-2}$·s$^{-1}$), irradiance at which the onset of light-saturated photosynthesis occurs; $\beta$, photoinhibition factor, 0 was set as the default value when there was no suppression. The values are shown as mean ± standard deviation ($n$ = 3). Different letters denote significantly different means across the groups ($P$ < 0.05).

| | N-limited cells | | Energy-limited cells | |
|---|---|---|---|---|
| **Parameters** | **$NO_3^-$** | **$NH_4^+$** | **$NO_3^-$** | **$NH_4^+$** |
| rETR(II)$_{max}$ | 149$^a$ ± 14 | 150$^a$ ± 8 | 104$^b$ ± 7 | 97.0$^b$ ± 7.0 |
| $\alpha$ | 0.17$^a$ ± 0.02 | 0.17$^a$ ± 0.01 | 0.11$^b$ ± 0.01 | 0.12$^b$ ± 0.01 |
| $E_k$ | 895$^a$ ± 123 | 880$^a$ ± 21 | 929$^a$ ± 97 | 797$^a$ ± 97 |
| $\beta$ | -0.02$^a$ ± 0.01 | -0.03$^a$ ± 0.00 | 0 | 0 |

**Table 4.** *Kinetic parameters of the rETR(I) versus irradiance curve in the presence or absence 5 µM DCMU of* Synechococcus *sp. UTEX LB 2380 acclimated to N- or energy-limited conditions, in the presence of either $NO_3^-$ or $NH_4^+$, at an irradiance of 100 µmol photons·m$^{-2}$·s$^{-1}$*

rETRmax, maximum relative electron transport rate; $\alpha$, slope of the light-limited portion of the rETR versus irradiance curve; $E_k$, irradiance at which the onset of light saturation photosynthesis occurs; $\beta$, photoinhibition factor, 0 was set as the default value when there was no suppression. The values are shown as mean ± standard deviations ($n$ = 3). Different letters denote significantly different means across the groups ($P$ < 0.05).

| | N-limited cells | | Energy-limited cells | |
|---|---|---|---|---|
| **Parameters** | **$NO_3^-$** | **$NH_4^+$** | **$NO_3^-$** | **$NH_4^+$** |
| rETR(I)$_{max}$ | 390$^a$ ± 33 | 383$^a$ ± 6 | 496$^b$ ± 54 | 656$^c$ ± 63 |
| +5 µM DCMU | 91$^{ab}$ ± 43 | 49$^b$ ± 13 | 89$^a$ ± 16 | 50$^b$ ± 11 |
| $\alpha$ | 0.59$^a$ ± 0.13 | 0.55$^a$ ± 0.08 | 0.30$^b$ ± 0.01 | 0.37$^c$ ± 0.00 |
| +5 µM DCMU | 0.66$^a$ ± 0.11 | 0.59$^a$ ± 0.10 | 0.42$^b$ ± 0.05 | 0.60$^a$ ± 0.05 |
| $E_k$ | 834$^a$ ± 163 | 710$^a$ ± 96 | 1648$^b$ ± 186 | 1757$^b$ ± 151 |
| +5 µM DCMU | 134$^{ab}$ ± 60 | 82$^a$ ± 9 | 199$^b$ ± 50 | 103$^{ab}$ ± 37 |
| $\beta$® | -0.04$^a$ ± 0.02 | -0.07$^a$ ± 0.01 | 0 | 0 |
| +5 µM DCMU | -0.08$^a$ ± 0.08 | -0.04$^a$ ± 0.03 | -0.04$^a$ ± 0.01 | -0.02$^a$ ± 0.02 |

## Discussion

Cell growth and reproduction ultimately depend on C assimilation. C assimilation cannot prescind from C acquisition. However, growth also requires the assimilation of other nutrients, and especially N, which, in a cell, is the second most abundant nutrient after C. We thus expect that energy partitioning between C and N acquisition and assimilation are interlinked (Kaffes *et al.,* 2010). In this work we addressed the problem of how the availability of different N chemical forms affects energy allocation to C acquisition and assimilation. In the experimental organism used for this study, C acquisition is mediated by a CCM (Tu *et al.,* 1987; Spiller *et al.,* 1988; Badger *et al.,* 1998; Price *et al.,* 2004, 2008). When energy limits growth, C and N assimilation may compete for energy. This competition, however, may be more or less accentuated depending on the N chemical form that is available and on the amount of energy required for its assimilation (Lara and Romero, 1986; Romero and Lara, 1987). We hypothesized that when N is available as $NH_4^+$ rather than $NO_3^-$, so that there is no diversion of energy to $NO_3^-$ reduction, more energy can be allocated to C assimilation and to the CCM that supplies intracellular $CO_2$.

When energy was limiting, the higher energy available to cells grown on $NH_4^+$ caused more rapid Ci assimilation and a faster growth rate (Fig. 1; Table 1). This agrees with the higher productivity, in terms of both biomass (dry weight) and organic C, observed in $NH_4^+$-grown cells by Ruan and Giordano (2017). When N was limiting (and energy was sufficient or in excess), the difference in the Ci affinity between $NH_4^+$- and $NO_3^-$-grown cells disappeared. Somewhat surprisingly, even when energy was not limiting, $NH_4^+$-grown cells maintained a larger internal Ci pool than their $NO_3^-$-grown counterparts (Fig. 3). This may be related to the CCM dissipating excessive energy by increased leakage of $CO_2$ down a larger free energy gradient from a higher intracellular $CO_2$ concentration. Greater energy dissipation would be needed more under N limitation (when energy is in excess) and especially in $NH_4^+$-grown cells, which cannot use $NO_3^-$ reduction as an electron sink. This agrees with the pivotal role of cyanobacterial CCMs in keeping the photosynthetic reaction centres open under excess irradiance, and so lessening photodamage, described by de Araujo *et al.,* (2011) for *Leptolyngbya*

sp. In energy-limited cells, the dissipation of energy may not be relevant. It is also noteworthy that, for a given N source, internal Ci pools of similar size were determined for energy- and N-limited cells, in spite of a much higher rate of $CO_2$ consumption by photosynthesis (measured as a 41% higher rate of $O_2$ evolution) in energy-limited cells. This suggests that, under energy limitation, a larger quota of energy is devoted to building-up the internal Ci pool than under N limitation, given that sustaining higher assimilation rates with a constant intracellular Ci pool can only be achieved by a higher pumping rate (Tchernov *et al.,* 1997, 2003) or by lower efflux rates (leakage; Tchernov *et al.,* 1997; Qiu and Liu, 2004; de Araujo *et al.,* 2011). Furthermore, in energy-limited cells, using the energetically cheaper N source $NH_4^+$ allowed cells to divert the energy saved to the CCM (greater Ci pool and higher photosynthetic affinity for Ci) and C fixation (higher photosynthetic rates), and, ultimately, growth (higher specific growth rate, μ). The same does not happen when N is limiting growth and the energy supply is sufficient or in excess. Our hypothesis is thus supported by our experimental data. The finding that the internal (cytosol) pH of cells grown on $NH_4^+$ was higher than that of cells grown on $NO_3^-$ when energy was limiting for growth (Table 2) contrasts with the prediction of a lower cytosol pH when $NH_4^+$ (at non-toxic concentrations) rather than $NO_3^-$ is the N source (Raven and De Michelis, 1979, 1980), but the lack of effect of N source on cytosol pH when energy is not limiting agrees with the findings of Raven and De Michelis (1979, 1980).

Increased expression of the $Na^+/HCO_3^-$ transporter, CA, and carboxysome protein have been reported for cells grown on $NH_4^+$ rather than on $NO_3^-$ (Ludwig and Bryant, 2012). In our study we did not assess the quantity of CCM components; however, the increase of the cell quotas of Fe and Zn found in the course of this work does agree with an increased abundance of Zn-CAs involved in the CCM (Fig. 4; Blindauer, 2008) and a higher photosynthetic activity (the requirement of Fe in the Fe-S centres of cytochrome b6f and PSI is known to be very high; Fig. 4; Raven, 1990). However, the Fe requirement for $NO_3^-$ reductase and, especially, $NO_2^-$ reductase is absent from $NH_4^+$-grown cells (Raven, 1990). These changes were only visible when energy was limiting, further confirming that the impact of the N chemical form on cell responses is linked to the energy demand for N assimilation.

The response of photosynthetic electron transfer to the growth treatments is somewhat puzzling: the N source had no impact on rETR(II) but, when energy was limiting, $NH_4^+$ stimulated rETR(I). The causes of this pattern could be various: the assimilation of $NH_4^+$ requires a lower $e^-$/ATP ratio than does $NO_3^-$ assimilation, consistent with the stimulation of rETR(I) in energy-limited $NH_4^+$-grown cells as a result of a relatively greater cyclic electron transfer around PSI. However, when PSII activity was inhibited by DCMU, rETR(I) became lower in $NH_4^+$, both in N- and in energy-limited cells. This suggests that (1) growth in the presence of $NH_4^+$ does not require a higher rate of cyclic electron transfer, and (2) cyclic electron transfer is not affected by energy availability. The interpretation of these data is made more difficult by the fact that, in cyanobacteria, the NAD(P)H-quinone oxidase, the cytochrome $b_6f$ complex, and the soluble cytochrome *c* or plastocyanin are shared by the photosynthetic and the respiratory electron transport chains. It can therefore not be excluded that the persistence of rETR(I) after DCMU treatment was due to an overflow of electrons from respiration (Kranz *et al.,* 2011). If this occurred only in energy-limited cells, it could have been the consequence of a higher electron demand for $NO_3^-$ reduction; however, given that the same phenomenon was also seen in N-limited cells, this option is rather unlikely. Based on all the above, it seems legitimate to conclude that the lower rETR(II) and a higher rETR(I), especially when the N source was $NH_4^+$, was due to a state transition that diverted more energy towards PSI when energy was in scarce supply, and especially in the presence of $NH_4^+$. This would not lead to a higher ratio of ATP to reducing power, as would be expected for $NH_4^+$ assimilation, but rather to a stimulation of the production of reducing power. This seems to fit with the hypothesis of an overflow of energy from N assimilation to Ci acquisition and assimilation, which are indeed higher in the conditions in which rETR(I) is higher. This interpretation agrees with linear photosynthetic electron transfer powering $Na^+$-dependent $HCO_3^-$ transporters of cyanobacterial CCMs (Li and Canvin, 1998), and with the observation by Ludwig and Bryant (2012) that the expression of SbtA was more than 3-fold higher when $NH_4^+$ rather than $NO_3^-$ was the N source. Also, the NDH-$1_3$ and NDH-$1_4$ complexes, which energize the irreversible conversion of $CO_2$ to $HCO_3^-$ as part of the CCM (Badger and Price, 2003; Price *et al.,* 2008), are more highly expressed with $NH_4^+$ than with a $NO_3^-$ as the N source (Ludwig and Bryant, 2012). NDH-$1_4$, which is usually constitutive and has a rather low affinity for $CO_2$, appears to be energized by PSI cyclic electron transfer (Maeda *et al.,* 2002); NDH-$1_3$, which is strongly inducible and has a high affinity for $CO_2$, has higher expression in $NH_4^+$-grown cells than does NDH-$1_4$, and is energized by linear electron transfer (Maeda *et al.,* 2002). The location of NDH-$1_4$ is not clear, but if (as indicated in figure 2 of Price, 2011) it is in the plasmalemma, the dependence on linear photosynthetic electron transfer could involve reduced ferredoxin or NADPH from linear electron transport supplying a respiratory chain involving NDH-$1_4$. These findings are also compatible with the idea that the higher linear electron transfer rate of energy-limited $NH_4^+$-grown cells is associated with a higher CCM activity of these cells.

## Conclusions

The data reported in this paper and the arguments used in the discussion appear to support the hypothesis that the energy saved by the use of the more reduced combined form of N ($NH_4^+$) under energy limitation is diverted towards C acquisition. What is known of the natural habitat of *Synechococcus* UTEX LB 2380 suggests that $NH_4^+$ is the dominant form of inorganic N; therefore the ability of the CCM to use the energy not required in the assimilation of oxidized N may represent a non-trivial advantage in the real world.

## Supplementary data

Supplementary data are available at *JXB* online.

**Table S1.** Carbonate system in the culture media at 25°C.

**Table S2.** Determination coefficients ($R^2$) of the goodness-of-fit of the linear models applied to the double-reciprocal plots and the DIC-limited part (*slope*) of photosynthesis versus DIC curves.

**Fig. S1.** Relative electron transport rate (rETR) at PSI and PSII versus irradiance curves under different conditions.

**Fig. S2.** Relative electron transfer rate versus irradiance curves for *Synechococcus* sp. UTEX LB 2380 cultured in the presence of 550 µM $NO_3^-$ or $NH_4^+$, at an irradiance of 100 µmol photons·$m^{-2}$·$s^{-1}$.

**Fig. S3.** (**A**) Linear $rETR_{max}$ and (**B**) per cent contribution of linear rETR to total rETR(I) for *Synechococcus* sp. UTEX LB 2380 acclimated to 22 or 550 µM of either $NO_3^-$ or $NH_4^+$ at an irradiance of 100 µmol photons·$m^{-2}$·$s^{-1}$; (**C**) the affinity for photons of rETR(I) and (**D**) the per cent increase in affinity for photons of rETR(I) resulting from addition of DCMU.

## Acknowledgements

We thank Antonio Pusceddu for his help for the statistical analyses. This work was funded by grant 27-12-2011 MAE-MOST and by grants GIO2010 and GIO2011 Ricerca Scientifica di Ateneo UNIVPM, all to M.G. The University of Dundee is a registered Scottish Charity, No SC 015096.

## References

**Acuña AM, Snellenburg JJ, Gwizdala M, Kirilovsky D, van Grondelle R, van Stokkum IH.** 2016. Resolving the contribution of the uncoupled phycobilisomes to cyanobacterial pulse-amplitude modulated (PAM) fluorometry signals. Photosynthesis Research **127,** 91–102.

**Badger MR, Andrews TJ.** 1982. Photosynthesis and inorganic carbon usage by the marine cyanobacterium, *Synechococcus* sp. Plant Physiology **70,** 517–523.

**Badger MR, Andrews TJ, Whitney S, Ludwig M, Yellowlees DC, Leggat W, Price GD.** 1998. The diversity and coevolution of Rubisco, plastids, pyrenoids, and chloroplast-based $CO_2$-concentrating mechanisms in algae. Canadian Journal of Botany **76,** 1052–1071.

**Badger MR, Price GD.** 2003. $CO_2$ concentrating mechanisms in cyanobacteria: molecular components, their diversity and evolution. Journal of Experimental Botany **54,** 609–622.

**Bartual A, Gálvez J.** 2002. Growth and biochemical composition of the diatom *Phaeodactylum tricornutum* at different pH and inorganic carbon levels under saturating and subsaturating light regimes. Botanica Marina **45,** 491–501.

**Beardall J.** 1991. Effects of photon flux density on the '$CO_2$ concentrating mechanism' of the cyanobacterium *Anabaena variabilis*. Journal of Plankton Research **13,** 133–141.

**Beardall J, Giordano M.** 2002. Ecological implications of microalgal and cyanobacterial $CO_2$ concentrating mechanisms and their regulation. Functional Plant Biology **29,** 335–347.

**Blindauer CA.** 2008. Zinc-handling in cyanobacteria: an update. Chemistry & Biodiversity **5,** 1990–2013.

**Campbell D, Hurry V, Clarke AK, Gustafsson P, Oquist G.** 1998. Chlorophyll fluorescence analysis of cyanobacterial photosynthesis and acclimation. Microbiology and Molecular Biology Reviews: MMBR **62,** 667–683.

**Cavet JS, Borrelly GP, Robinson NJ.** 2003. Zn, Cu and Co in cyanobacteria: selective control of metal availability. FEMS Microbiology Reviews **27,** 165–181.

**Coronil T, Lara C, Guerrero MG.** 1993. Shift in carbon flow and stimulation of amino-acid turnover induced by nitrate and ammonium assimilation in *Anacystis nidulans*. Planta **189,** 461–467.

**de Araujo ED, Patel J, de Araujo C, Rogers SP, Short SM, Campbell DA, Espie GS.** 2011. Physiological characterization and light response of the $CO_2$-concentrating mechanism in the filamentous cyanobacterium *Leptolyngbya* sp. CPCC 696. Photosynthesis Research **109,** 85–101.

**Dickson AG.** 1990. Standard potential of the reaction: AgCl (s) + $12H_2$ (g) = Ag (s) + HCl (aq), and and the standard acidity constant of the ion $HSO_4^-$ in synthetic sea water from 273.15 to 318.15 K. The Journal of Chemical Thermodynamics **22,** 113–127.

**DiMario RJ, Clayton H, Mukherjee A, Ludwig M, Moroney JV.** 2017. Plant carbonic anhydrases: structures, locations, evolution, and physiological roles. Molecular Plant **10,** 30–46.

**Fanesi A, Raven JA, Giordano M.** 2014. Growth rate affects the responses of the green alga *Tetraselmis suecica* to external perturbations. Plant, Cell and Environment **37,** 512–519.

**Fu X, Han B.** 2010. Response of cyanobacterial carbon concentrating system to light intensity: a simulated analysis. Chinese Journal of Oceanology and Limnology **28,** 478–488.

**Fukuzawa H, Ogawa T, Kaplan A.** 2012. The uptake of $CO_2$ by cyanobacteria and microalgae. In: **Eaton-Rye JJ, Tripathy BC, Sharkey TD**, eds. Photosynthesis, Vol. 34. Dordrecht: Springer Netherlands, 625–650.

**Giordano M.** 2001. Interactions between C and N metabolism in *Dunaliella salina* cells cultured at elevated $CO_2$ and high N concentrations. Journal of Plant Physiology **158,** 577–581.

**Giordano M, Beardall J, Raven JA.** 2005. $CO_2$ concentrating mechanisms in algae: mechanisms, environmental modulation, and evolution. Annual Review of Plant Biology **56,** 99–131.

**Giordano M, Bowes G.** 1997. Gas exchange and C allocation in *Dunaliella salina* cells in response to the N source and $CO_2$ concentration used for growth. Plant Physiology **115,** 1049–1056.

**Huppe H, Turpin D.** 1994. Integration of carbon and nitrogen metabolism in plant and algal cells. Annual Review of Plant Biology **45,** 577–607.

**Kaffes A, Thoms S, Trimborn S, Rost B, Langer G, Richter KU, Köhler A, Norici A, Giordano M.** 2010. Carbon and nitrogen fluxes in the marine coccolithophore *Emiliania huxleyi* grown under different nitrate concentrations. Journal of Experimental Marine Biology and Ecology **393,** 1–8.

**Kaplan A, Ronen-Tarazi M, Zer H, Schwarz R, Tchernov D, Bonfil DJ, Schatz D, Vardi A, Hassidim M, Reinhold L.** 1998. The inorganic carbon-concentrating mechanism in cyanobacteria: induction and ecological significance. Canadian Journal of Botany **76,** 917–924.

**Kaplan A, Zenvirth D, Marcus Y, Omata T, Ogawa T.** 1987. Energization and activation of inorganic carbon uptake by light in cyanobacteria. Plant Physiology **84,** 210–213.

**Kerfeld CA, Melnicki MR.** 2016. Assembly, function and evolution of cyanobacterial carboxysomes. Current Opinion in Plant Biology **31,** 66–75.

**Kerfeld CA, Sawaya MR, Tanaka S, Nguyen CV, Phillips M, Beeby M, Yeates TO.** 2005. Protein structures forming the shell of primitive bacterial organelles. Science **309,** 936–938.

**Klughammer C, Schreiber U.** 1994. An improved method, using saturating light pulses, for the determination of photosystem I quantum yield via $P700^+$ absorbance changes at 830 nm. Planta **192,** 261–268.

**Kranz SA, Eichner M, Rost B.** 2011. Interactions between CCM and $N_2$ fixation in Trichodesmium. Photosynthesis Research **109,** 73–84.

**Kübler JE, Raven JA.** 1994. Consequences of light limitation for carbon acquisition in three rhodophytes. Marine Ecology Progress Series **110,** 203–209.

**Kübler JE, Raven JA.** 1995. The interaction between inorganic carbon acquisition and light supply in *Palmaria palmata* (Rhodophyta). Journal of Phycology **31,** 369–375.

**Kupriyanova E, Villarejo A, Markelova A, Gerasimenko L, Zavarzin G, Samuelsson G, Los DA, Pronina N.** 2007. Extracellular carbonic anhydrases of the stromatolite-forming cyanobacterium *Microcoleus chthonoplastes*. Microbiology **153,** 1149–1156.

**Lara C, Romero JM.** 1986. Distinctive light and $CO_2$-fixation requirements of nitrate and ammonium utilization by the cyanobacterium *Anacystis nidulans*. Plant Physiology **81,** 686–688.

**Lawrie AC, Codd GA, Stewart WD.** 1976. The incorporation of nitrogen into products of recent photosynthesis in *Anabaena cylindrica* Lemm. Archives of Microbiology **107,** 15–24.

**Lewis E, Wallace D, Allison LJ.** 1998. Program developed for $CO_2$ system calculations: Carbon Dioxide Information Analysis Center, managed by Lockheed Martin Energy Research Corporation for the US Department of Energy Tennessee. http://cdiac.esd.ornl.gov/oceans/co2rprtnbk, last accessed 13 March 2017.

**Li Q, Canvin DT.** 1998. Energy sources for $HCO_3^-$ and $CO_2$ transport in air-grown cells of *Synechococcus* UTEX 625. Plant Physiology **116,** 1125–1132.

**López-Igual R, Picossi S, López-Garrido J, Flores E, Herrero A.** 2012. N and C control of ABC-type bicarbonate transporter Cmp and its LysR-type transcriptional regulator CmpR in a heterocyst-forming cyanobacterium, *Anabaena* sp. Environmental Microbiology **14,** 1035–1048.

**Ludwig M, Bryant DA.** 2012. Acclimation of the global transcriptome of the cyanobacterium *Synechococcus* sp. strain PCC 7002 to nutrient limitations and different nitrogen sources. Frontiers in Microbiology **145,** 1–15.

**Maeda S, Badger MR, Price GD.** 2002. Novel gene products associated with NdhD3/D4-containing NDH-1 complexes are involved in photosynthetic $CO_2$ hydration in the cyanobacterium, *Synechococcus* sp. PCC7942. Molecular Microbiology **43,** 425–435.

**McGurn LD, Moazami-Goudarzi M, White SA, Suwal T, Brar B, Tang JQ, Espie GS, Kimber MS.** 2016. The structure, kinetics and interactions of the β-carboxysomal β-carbonic anhydrase, CcaA. The Biochemical Journal **473,** 4559–4572.

**Mi H, Endo T, Ogawa T, Asada K.** 1995. Thylakoid membrane-bound, NADPH-specific pyridine nucleotide dehydrogenase complex mediates cyclic electron transport in the cyanobacterium *Synechocystis* sp. PCC 6803. Plant and Cell Physiology **36,** 661–668.

**Mi H, Endo T, Schreiber U, Ogawa T, Asada K.** 1992. Electron donation from cyclic and respiratory flows to the photosynthetic intersystem chain is mediated by pyridine nucleotide dehydrogenase in the cyanobacterium *Synechocystis* PCC 6803. Plant and Cell Physiology **33,** 1233–1237.

**Michaelis L, Menten ML.** 1913. Die kinetik der invertinwirkung. Biochemische Zeitschrift **49,** 333–369.

**Miller AG, Espie GS, Canvin DT.** 1988. Active transport of $CO_2$ by the cyanobacterium *Synechococcus* UTEX 625: measurement by mass spectrometry. Plant Physiology **86,** 677–683.

**Millero FJ.** 1995. Thermodynamics of the carbon dioxide system in the oceans. Geochimica et Cosmochimica Acta **59,** 661–677.

**Neall VE, Trewick SA.** 2008. The age and origin of the Pacific islands: a geological overview. Philosophical Transactions of the Royal Society of London. Series B, Biological Sciences **363,** 3293–3308.

**Noctor G, Foyer CH.** 1998. A re-evaluation of the ATP: NADPH budget during $C_3$ photosynthesis: a contribution from nitrate assimilation and its associated respiratory activity? Journal of Experimental Botany **49,** 1895.

**Omata T, Price GD, Badger MR, Okamura M, Gohta S, Ogawa T.** 1999. Identification of an ATP-binding cassette transporter involved in bicarbonate uptake in the cyanobacterium *Synechococcus* sp. strain PCC 7942. Proceedings of the National Academy of Sciences **96,** 13571–13576.

**Pfündel E, Klughammer C, Schreiber U.** 2008. Monitoring the effects of reduced PSII antenna size on quantum yields of photosystems I and II using the Dual-PAM-100 measuring system. PAM Application Notes **1,** 21–24.

**Poza-Carrión C, Fernández-Valiente E, Piñas FF, Leganés F.** 2001. Acclimation of photosynthetic pigments and photosynthesis of the cyanobacterium *Nostoc* sp. strain UAM206 to combined fluctuations of irradiance, pH, and inorganic carbon availability. Journal of Plant Physiology **158,** 1455–1461.

**Price GD.** 2011. Inorganic carbon transporters of the cyanobacterial $CO_2$ concentrating mechanism. Photosynthesis Research **109,** 47–57.

**Price GD, Badger MR, Woodger FJ, Long BM.** 2008. Advances in understanding the cyanobacterial $CO_2$-concentrating-mechanism (CCM): functional components, Ci transporters, diversity, genetic regulation and prospects for engineering into plants. Journal of Experimental Botany **59,** 1441–1461.

**Price GD, Woodger FJ, Badger MR, Howitt SM, Tucker L.** 2004. Identification of a SulP-type bicarbonate transporter in marine cyanobacteria. Proceedings of the National Academy of Sciences U S A **101,** 18228–18233.

**Qiu B, Liu J.** 2004. Utilization of inorganic carbon in the edible cyanobacterium Ge-Xian-Mi (*Nostoc*) and its role in alleviating photo-inhibition. Plant, Cell and Environment **27,** 1447–1458.

**Ratti S, Giordano M, Morse D.** 2007. $CO_2$-concentrating mechanisms of the potentially toxic dinoflagellate *Protoceratium reticulatum* (Dinophyceae, Gonyaulacales). Journal of Phycology **43,** 693–701.

**Ratti S, Knoll AH, Giordano M.** 2011. Did sulfate availability facilitate the evolutionary expansion of chlorophyll a+c phytoplankton in the oceans? Geobiology **9,** 301–312.

**Raven JA.** 1990. Predictions of Mn and Fe use efficiencies of phototrophic growth as a function of light availability for growth and of C assimilation pathway. New Phytologist **116,** 1–18.

**Raven J, Beardall J.** 2014. $CO_2$ concentrating mechanisms and environmental change. Aquatic Botany **118,** 24–37.

**Raven JA, Beardall J.** 2016. Algal photosynthesis and physiology. In: **Slocombe SP, Benemann JR**, eds. Microalgal production for biomass and high-value products. London: Taylor & Francis Group, 1–20.

**Raven JA, Beardall J, Giordano M.** 2014. Energy costs of carbon dioxide concentrating mechanisms in aquatic organisms. Photosynthesis Research **121,** 111–124.

**Raven J, De Michelis M.** 1979. Acid-base regulation during nitrate assimilation in *Hydrodictyon africanum*. Plant, Cell and Environment **2,** 245–257.

**Raven J, De Michelis M.** 1980. Acid-base regulation during ammonium assimilation in *Hydrodictyon africanum*. Plant, Cell and Environment **3,** 325–338.

**Raven JA, Giordano M, Beardall J, Maberly SC.** 2011. Algal and aquatic plant carbon concentrating mechanisms in relation to environmental change. Photosynthesis Research **109,** 281–296.

**Raven JA, Giordano M, Beardall J, Maberly SC.** 2012. Algal evolution in relation to atmospheric $CO_2$: carboxylases, carbon-concentrating mechanisms and carbon oxidation cycles. Philosophical Transactions of the Royal Society of London. Series B, Biological Sciences **367,** 493–507.

**Raven J, Lucas W.** 1985. Energy costs of carbon acquisition. In: **Lucas W, Berry J**, eds. Inorganic carbon uptake by aquatic photosynthetic organism. Davis, CA: The American Society of Plant Physiologists, 305–324.

**Romero JM, Lara C.** 1987. Photosynthetic assimilation of $NO_3^-$ by intact cells of the cyanobacterium *Anacystis nidulans*: influence of $NO_3^-$ and $NH_4^+$ assimilation on $CO_2$ fixation. Plant Physiology **83,** 208–212.

**Roy RN, Roy LN, Vogel KM, Porter-Moore C, Pearson T, Good CE, Millero FJ, Campbell DM.** 1993. The dissociation constants of carbonic acid in seawater at salinities 5 to 45 and temperatures 0 to 45°C. Marine Chemistry **44,** 249–267.

**Ruan Z, Giordano M.** 2017. The use of $NH_4^+$ rather than $NO_3^-$ affects cell stoichiometry, C allocation, photosynthesis and growth in the cyanobacterium *Synechococcus* sp. UTEX LB 2380, only when energy is limiting. Plant, Cell and Environment **40,** 227–236.

**Salon C, Mir N, Canvin D.** 1996. Influx and efflux of inorganic carbon in *Synechococcus* UTEX625. Plant, Cell and Environment **19,** 247–259.

**Schreiber U, Klughammer C.** 2008. Saturation pulse method for assessment of energy conversion in PSI. PAM Application Notes **1,** 11–14.

**Scott K, Henn-Sax M, Harmer T, Longo D, Frame C, Cavanaugh C.** 2007. Kinetic isotope effect and biochemical characterization of form IA RubisCO from the marine cyanobacterium *Prochlorococcus marinus* MIT9313. Limnology and Oceanography **52,** 2199–2204.

**Shamberger KEF, Cohen AL, Golbuu Y, McCorkle DC, Lentz SJ, Barkley HC.** 2014. Diverse coral communities in naturally acidified waters of a Western Pacific reef. Geophysical Research Letters **41,** 499–504.

**Shibata M, Katoh H, Sonoda M, Ohkawa H, Shimoyama M, Fukuzawa H, Kaplan A, Ogawa T.** 2002. Genes essential to sodium-dependent bicarbonate transport in cyanobacteria: function and phylogenetic analysis. The Journal of Biological Chemistry **277,** 18658–18664.

**Spiller H, Wynns GC, Tu C.** 1988. Role of photosynthetic reactions in the activity of carbonic anhydrase in *Synechococcus* sp. (UTEX 2380) in

the light: inhibitor studies using the $^{18}O$-exchange in $^{13}C/^{18}O$-labeled bicarbonate. Plant Physiology **86,** 1185–1192.

**Stitt M, Krapp A.** 2002. The interaction between elevated carbon dioxide and nitrogen nutrition: the physiological and molecular background. Plant, Cell and Environment **22,** 583–621.

**Suggett DJ, MacIntyre HL, Kana TM, Geider RJ.** 2009. Comparing electron transport with gas exchange: parameterising exchange rates between alternative photosynthetic currencies for eukaryotic phytoplankton. Aquatic Microbial Ecology **56,** 147–162.

**Suggett DJ, Oxborough K, Baker NR, MacIntyre HL, Kana TM, Geider RJ.** 2003. Fast repetition rate and pulse amplitude modulation chlorophyll a fluorescence measurements for assessment of photosynthetic electron transport in marine phytoplankton. European Journal of Phycology **38,** 371–384.

**Taylor J.** 1997. Introduction to error analysis, the study of uncertainties in physical measurements (2nd edition). New York: University Science Books.

**Tchernov D, Hassidim M, Luz B, Sukenik A, Reinhold L, Kaplan A.** 1997. Sustained net $CO_2$ evolution during photosynthesis by marine microorganisms. Current Biology **7,** 723–728.

**Tchernov D, Silverman J, Luz B, Reinhold L, Kaplan A.** 2003. Massive light-dependent cycling of inorganic carbon between oxygenic photosynthetic microorganisms and their surroundings. Photosynthesis Research **77,** 95–103.

**Tortell PD.** 2000. Evolutionary and ecological perspectives on carbon acquisition in phytoplankton. Limnology and Oceanography **45,** 744–750.

**Tu C, Spiller H, Wynns GC, Silverman DN.** 1987. Carbonic anhydrase and the uptake of inorganic carbon by *Synechococcus* sp. (UTEX-2380). Plant Physiology **85,** 72–77.

**Walsby AE.** 1997. Modelling the daily integral of photosynthesis by phytoplankton: its dependence on the mean depth of the population. Hydrobiologia **349,** 65–74.

**Watanabe A, Kayanne H, Hata H, Kudo S, Nozaki K, Kato K, Negishi A, Ikeda Y, Yamano H.** 2006. Analysis of the seawater $CO_2$ system in the barrier reef - lagoon system of Palau using total alkalinity - dissolved inorganic carbon diagrams. Limnology and Oceanography **51,** 1614–1628.

**Ye C, Gao K, Giordano M.** 2008. The odd behaviour of carbonic anhydrase in the terrestrial cyanobacterium *Nostoc flagelliforme* during hydration-dehydration cycles. Environmental Microbiology **10,** 1018–1023.

**Zhang P, Battchikova N, Jansen T, Appel J, Ogawa T, Aro EM.** 2004. Expression and functional roles of the two distinct NDH-1 complexes and the carbon acquisition complex NdhD3/NdhF3/CupA/Sll1735 in *Synechocystis* sp PCC 6803. The Plant Cell **16,** 3326–3340.